


S.O. KONOROV¹,
A.A. IVANOV²,
M.V. ALFIMOV²,
A.M. ZHELTIKOV^{1,3}, 

Polarization-sensitive non- 3ω third-harmonic generation by femtosecond Cr: Forsterite laser pulses in birefringent microchannel waveguides of photonic-crystal fibers

¹Physics Department, M.V. Lomonosov Moscow State University, Vorob'evy gory, 119992 Moscow, Russia

²Center of Photochemistry, Russian Academy of Sciences, Novatorov 7a, 117421 Moscow, Russia

³International Laser Center, M.V. Lomonosov Moscow State University, Vorob'evy gory, 119992 Moscow, Russia

Received: 28 January 2005

Published online: 15 July 2005 • © Springer-Verlag 2005

ABSTRACT Femtosecond Cr: forsterite laser pulses coupled into small-diameter birefringent channel waveguides off the central core of a photonic-crystal fiber are shown to generate multiple narrowband spectral peaks within the 380–460 nm wavelength region through multimode-phase-matched third-harmonic generation. Some of these peaks are shifted by tens of terahertz from the tripled frequency of the pump field, dictated by standard energy conservation for third-harmonic generation in monochromatic fields. The spectral contents of the third-harmonic signal generated in such a regime are controlled by changing polarization and the intensity of the input pump field.

PACS 42.65.Wi; 42.81.Qb

1 Introduction

Photonic-crystal fibers (PCFs) [1–4] are giving a new momentum to the nonlinear optics of guided waves [5]. A radical enhancement of nonlinear-optical spectral transformations of laser pulses in PCFs, leading to a highly efficient supercontinuum generation [6–8] and frequency shifting [9–11], has allowed the creation of novel compact and convenient fiber-optic light sources for frequency metrology [12–15], biomedicine [16], photochemistry [17, 18], and ultrafast optics [19] as well as nonlinear spectroscopy [18, 20] and microscopy [21]. Due to their unique properties, PCFs have made it possible to observe new nonlinear-optical phenomena and novel interesting physical objects. Solid-core PCFs have been used to demonstrate a cancellation of the soliton self-frequency shift around the second zero group-velocity dispersion point [22] and self-induced modulation instability (MI) due to the third-order dispersion [23], while hollow-core PCFs permit the formation and nonlinear-optical transformations of isolated guided modes of high-intensity laser fields in the gas phase [24–28].

Third-harmonic generation (THG) in PCFs has received less attention than various types of parametric four-wave mixing (FWM) processes [29–31], partially because guided-mode phase-matching solutions, which are often nearly automatically satisfied or MI-induced for parametric FWM, are less obvious in the case of THG. Still, efficient THG has been recently observed in fused silica [32–37] and multicomponent-glass [38] PCFs, as well as in tapered fibers [39], offering interesting guided-mode [39] and Cherenkov-type [35, 38] phase-matching options. These experiments not only demonstrated the significance of THG for efficient, guided-wave frequency tripling of femtosecond laser pulses, but also revealed several new interesting features of this phenomenon. The third-harmonic signal has been shown to display an asymmetric spectral broadening [38, 39] or even a substantial frequency shift [37].

We will demonstrate in this work that intense spectral peaks shifted from the tripled frequency of the pump field, dictated by standard energy conservation for THG in monochromatic fields, are typical features of multimode guided-wave THG in the field of a short-pulse pump field. We will present the results of experiments showing that femtosecond Cr: forsterite laser pulses coupled into small-diameter birefringent channel waveguides off the central core of a PCF can generate multiple narrowband spectral peaks within the 380–460 nm wavelength region through multimode-phase-matched THG. We will demonstrate that the spectral contents of the third-harmonic signal generated in such a regime can be controlled by changing polarization and the intensity of the input pump field.

2 Phase matching for group-delayed guided-wave third-harmonic generation

In this section, we present a qualitative analysis of phase matching for THG in the waveguide regime taking into consideration the group-velocity mismatch of the pump and third-harmonic fields as well as nonlinear, intensity-dependent phase shifts of the pump and third-harmonic fields induced through self- and cross-phase

modulation. In this analysis, we neglect group-velocity dispersion and higher order dispersion effects as well as the self-phase modulation of the third-harmonic field. We represent the propagation constants β_p and β_h of guided modes at the frequencies of the pump field and the third harmonic as $\beta_p(\omega) \approx \beta_p(\omega_0) + v_p^{-1}\Omega/3 + \kappa_{\text{spm}}P$, $\beta_h(\omega) \approx \beta_h(3\omega_0) + v_h^{-1}\Omega + 2\kappa_{\text{xpm}}P$, where ω_0 is the central frequency of the pump field; $v_{p,h} = (\partial k/\partial \omega)_{\omega_0,3\omega_0}^{-1}$ are the group velocities of the pump and its third harmonic; $\Omega = 3\omega - 3\omega_0$; $\kappa_{\text{spm}} = \omega_0 n_2/c S_{\text{eff}}$ and $\kappa_{\text{xpm}} = 3\omega_0 \bar{n}_2/c S_{\text{eff}}$ are the SPM and XPM nonlinear coefficients (S_{eff} is the effective beam, or mode, area and n_2 and \bar{n}_2 are the nonlinear refractive indices at ω_0 and $3\omega_0$, respectively); and P is the peak power of the pump field. With $n_2 \approx \bar{n}_2$, the phase mismatch is then by $\Delta\beta = \beta_h - 3\beta_p \approx \Delta\beta_0 + \xi\Omega + 3\kappa_{\text{spm}}P$, where $\Delta\beta_0 = \beta_h(3\omega_0) - 3\beta_p(\omega_0)$ is the phase mismatch of the pump and third-harmonic propagation constants at the central frequencies of these fields and $\xi = v_h^{-1} - v_p^{-1}$ is the group-velocity mismatch.

In Fig. 1, we illustrate phase-matching options for multi-mode THG in a fused silica fiber with a core radius of 1.2 μm (Fig. 1a) and 1.4 μm (Fig. 1b) and an air cladding. The material dispersion of fused silica is included in these calculations through the Sellmeier formula [40]. The central wavelength of the pump field is taken to be equal to the carrier wavelength of Cr: forsterite laser radiation, $\lambda_0 = 1.25 \mu\text{m}$. The nonlinear phase shifts are neglected. Curve 1 represent THG mismatches of propagation constants $\Delta\beta$ calculated by nu-

merically solving the relevant dispersion equation for the fundamental, HE_{11} mode of the pump field and the EH_{13} mode of the third harmonic. The propagation constant mismatch passes through zero around 0.40 μm in Fig. 1a and around 0.44 μm in Fig. 1b, indicating the possibility of phase-matched THG for the above-specified parameters of the fiber and the pump wavelength. Other phase-matching solutions are illustrated by curves 2 and 3, showing the phase mismatch for the fundamental mode of the pump field and the HE_{13} and EH_{42} eigenmodes, respectively. High-order third-harmonic modes can thus give rise to multiplets of spectral peaks in the spectrum of the third harmonic. A third-harmonic signal with such a spectral structure has been observed in our experiments, described in the following sections of this paper. The sign of the frequency shift of the phase-matched spectral component with respect to the central frequency $3\omega_0$, as illustrated by Fig. 1a and b for the $\text{HE}_{11} \rightarrow \text{EH}_{13}$ THG, can be switched by changing the core size by only 15% (0.2 μm in our case). This allows the spectral contents of the third-harmonic signal to be controlled by changing the size of the waveguiding channel in PCFs or by rotating polarization of the pump field in birefringent waveguides. The latter possibility will be illustrated by the experiments presented below in this paper.

The amplitudes of the spectral peaks corresponding to phase-matched THG generation in guided modes are determined by the length of nonlinear interaction, linear and nonlinear phase shifts, as well as by the intensity and the spectrum of the pump field [41, 42]. In the regime where the nonlinear phase shifts of the pump and third-harmonic fields are small, the spectrum of the third-harmonic intensity is given by [43]

$$I(\Omega, z) \propto \sigma^2 \sin^2 [(\Delta\beta_0 + \Omega\xi)z/2] (\Delta\beta_0 + \Omega\xi)^{-2} \times \left| \int_{-\infty}^{\infty} \int_{-\infty}^{\infty} A(\Omega - \Omega') A(\Omega' - \Omega'') A(\Omega'') d\Omega' d\Omega'' \right|^2,$$

where σ is the THG nonlinear coefficient and $A(\Omega)$ is the spectrum of the input pump field. In this regime, phase-matching effects can be decoupled from the influence of the spectrum of the pump field. While the phase matching is represented by the argument of the $\text{sinc}(x)$ function, entering the first factor of the expression for the spectrum of the third harmonic, the significance of the pump spectrum is clear from the convolution integral.

Depending on the signs of the phase and group-velocity mismatch, $\Delta\beta_0$ and ξ , the peak in the spectrum of the third harmonic can be either red- or blue-shifted with respect to the frequency $3\omega_0$. The spectral width of this peak, as can be seen from Eq. (15), is given by $\delta \approx 2\pi(|\xi|z)^{-1}$, decreasing as z^{-1} with the growth in the propagation coordinate z . The spectrum of the pump field, on the other hand, should be broad enough to provide a high amplitude of phase-matched peaks. Spectral shifts, limited to small Ω by a field-unperturbed pump spectrum and short interactions lengths, typical of nonlinear crystals, has been earlier predicted by Akhmanov et al. [44] for second-harmonic generation. Generation of high-amplitude well-resolved narrow-band third-harmonic peaks with large shifts Ω requires a mechanism for an efficient spectral

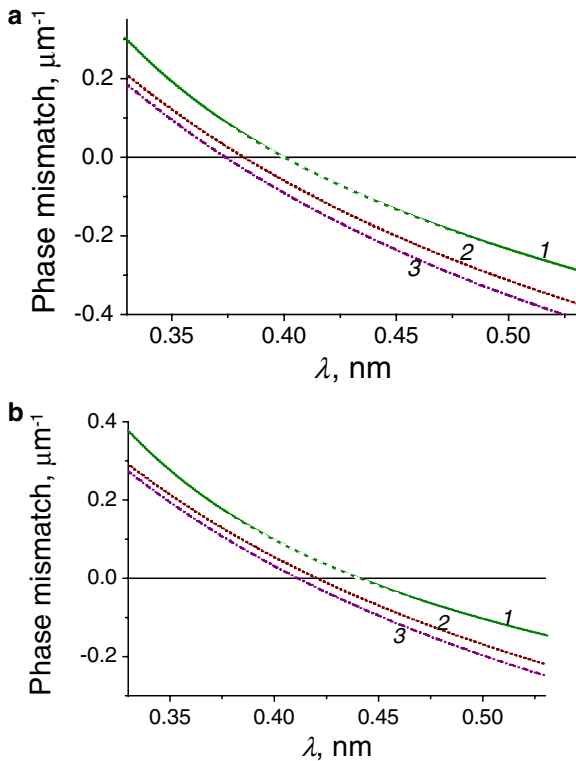


FIGURE 1 Mismatches of propagation constants $\Delta\beta$ for the THG process calculated for the fundamental, HE_{11} mode of the pump field and the EH_{13} (1), HE_{13} (2), and EH_{42} (3) modes of the third harmonic in a circular fiber with a fused silica core and an air cladding. The fiber core radius a is **a** 1.2 μm and **b** 1.4 μm . The central wavelength of the pump field is $\lambda_0 = 1.25 \mu\text{m}$

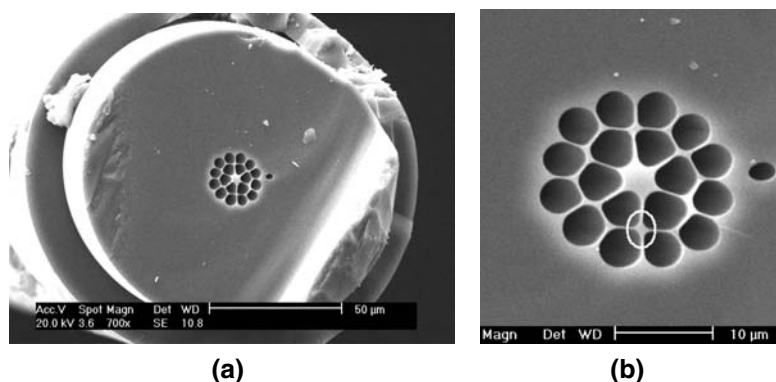


FIGURE 2 SEM images of the PCF. The scale bar corresponds to **a** 50 μm and **b** 10 μm . The ellipse labels a microchannel waveguide

broadening of the pump field. We show below that this requirement is fulfilled for THG in PCFs.

3 The laser system and PCF samples

The laser system used in our experiments consisted of a Cr^{4+} : forsterite master oscillator, a stretcher, an optical isolator, a regenerative amplifier, and a compressor. The master oscillator, pumped with a fiber ytterbium laser, generated 30–60 fs light pulses of radiation with a wavelength of 1.23–1.25 μm at a repetition rate of 120 MHz. These pulses were then transmitted through a stretcher and an isolator, to be amplified in a Nd:YLF-laser-pumped amplifier and recompressed to the 120 fs pulse duration with the maximum laser pulse energy up to 40 μJ at 1 kHz.

Photonic-crystal fibers used in our experiments were produced from fused silica using the standard technology [1–4, 10]. The fiber consisted of a solid core with a diameter of 4.3 μm , a microstructure cladding, which included two cycles of air holes, and an outer, solid part of the cladding. A cross-section view of the fiber is presented in Fig. 2. The light can be guided either through the central core of the PCF or through an array of small-size waveguide channels bounded by the air holes in the PCF cladding. One of such microchannel waveguides is marked with an ellipse in the close-up view of the PCF in Fig. 2b. A high refractive index step provides a strong confinement of the light field in these waveguides and supports multimode waveguiding regimes for a typical size of a channel of about 1 μm . Microchannel waveguides in the PCF, as can be seen from Fig. 2b, generally feature a noncircular shape of the cross section. This form anisotropy of channels was employed in our experiments for polarization switching of THG. Pump radiation of the Cr: forsterite laser was coupled into microchannel waveguides in our experiments with standard micro-objectives. The spectrum of radiation transmitted through the PCF was analyzed with an Ocean Optics spectrometer.

4 Results and discussion

Propagation of the pump pulse through the microchannel waveguide in the PCF is accompanied by nonlinear-optical transformations of its spectrum, induced by self-phase modulation, four-wave mixing, and soliton self-frequency shift. Figure 3 presents the spectra of unamplified pump pulses with an initial duration of about 60 fs

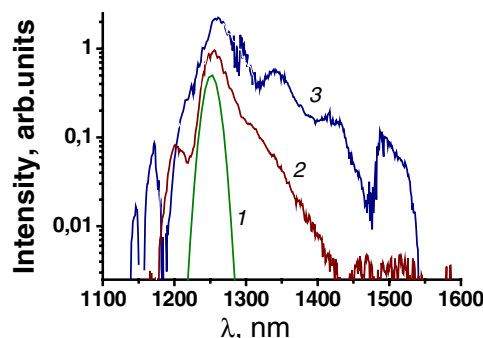


FIGURE 3 Spectral transformation of unamplified Cr, forsterite laser pulses transmitted through a microchannel waveguide in a 14 cm PCF. The initial pump pulse duration is 60 fs. The input spectrum of the pump field is shown by *curve 1*. The input pump pulse energy is 0.4 nJ (2) and 0.8 nJ (3)

transmitted through a PCF with a length of 14 cm. The pump field propagating through the microchannel waveguide channel in the regime of anomalous dispersion tends to form solitons, which experience red-shifting due to the Raman effect. This soliton self-frequency shift gives rise to the pronounced peaks in the long-wavelength part of the PCF-transformed pump spectrum in Fig. 3.

The spectrally broadened pump provides an ideal source for frequency shifted THG in microchannel waveguides in PCFs. Third-harmonic spectra measured at the output of the 14 cm PCF (Fig. 4) display well-resolved narrow-band peaks observed within the range of wavelengths from 370 to 460 nm, corresponding to approximately 170 THz in the frequency domain. The central wavelengths of these groups of peaks agree reasonably well with the results of phase-matching analysis, indicating phase-matched THG in higher order modes of the PCF. Rotating the linearly polarized pump field with respect to the short and long principal axes of the anisotropic microchannel waveguide (Fig. 2b), we observed shift switching of the dominant peak in the spectrum of the third harmonic. While the pump field oriented along the short axis of the waveguide cross section gives rise to an intense blue-shifted peak in the spectrum of the third harmonic (curve 1 in Fig. 4), a red-shifted peak dominates the spectrum of this signal in the regime when the pump field is polarized along the long axis of the microchannel waveguide (curve 2 in Fig. 4).

In the presence of a strong pump field, the THG phase-matching frequency shift Ω , as shown in Sect. 2, depends on the peak power P of the pump field, $\Omega(P) = -(\Delta\beta_0 + 3\kappa_{\text{spm}}P)/\xi$. For a typical situation of small-core

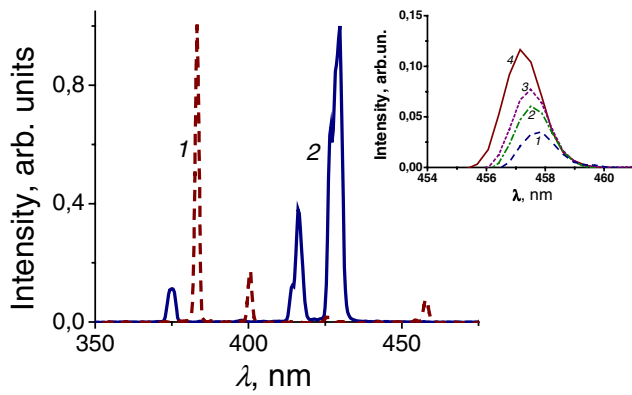


FIGURE 4 Spectra of the third harmonic generated by unamplified Cr: forsterite laser pulses with an initial duration of 60 fs in a microchannel waveguide of a 14 cm PCF. The linearly polarized pump field is oriented along the short (1) and long (2) principal axis of the waveguide cross section. The *inset* presents the spectra of one of the third-harmonic spectral components generated in a microchannel waveguide channel of a 10 cm PCF by unamplified 60-fs pump pulses with different input energies, (1) 0.5 nJ, (2) 0.7 nJ, (3) 0.9 nJ, and (4) 1.1 nJ

fused silica waveguide channels and PCFs with $\Delta\beta_0 > 0$, $\xi < 0$, and $\kappa_{\text{spm}} > 0$, the Kerr nonlinearity leads to a blue shifting of phase-matched peaks in the spectrum of the third harmonic with the growth in the pump intensity. This effect is observed for THG by unamplified 60 fs Cr: forsterite laser pulses in microchannel waveguides in PCFs. The increase in the input energy of pump pulses under these conditions as can be seen in the inset to Fig. 4, leads to a substantial blue-shifting of third-harmonic peaks, in accordance with the field-corrected phase-matching condition.

Amplified pump pulses of Cr: forsterite laser radiation induce much stronger phase shifts through the SPM and XPM effects. Frequency-shifted peaks in the spectrum of the third harmonic display a considerable broadening in this regime (Fig. 5), eventually merging together and forming a continuous band of blue emission spanning over more than 100 nm around the $3\omega_0$ frequency. This miniband around $3\omega_0$ substantially intensifies the short-wavelength wing in the spectrum of supercontinuum emission, which is efficiently generated in PCFs of the considered type by amplified femtosecond laser pulses. The main features and tendencies in pump-field-induced spectral broadening of the third harmonic generated in PCFs and tapered fibers by amplified femtosecond laser pulses have been earlier identified in [39, 42]. Images of the third-harmonic beam patterns at the output of the PCF (insets in Fig. 5) visualize spatial intensity profiles typical of high-order guided modes of the PCF. Similar high-order mode profiles have been earlier observed for the third harmonic of Ti: sapphire laser pump pulses generated in a high-index-step PCF [34].

5 Conclusion

We have shown in this paper that third-harmonic generation in the field of spectrally broadened short pump pulses can display interesting and practically significant new features. A short-pulse pump field broadened due to self-phase modulation can generate its third harmonic within a broad spectral range. However, the phase-matching condition gen-

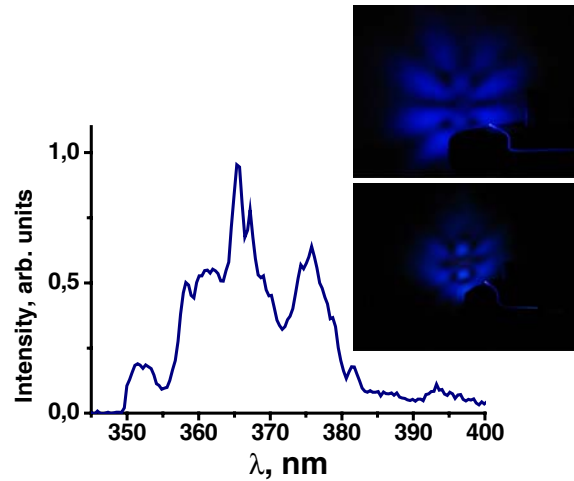


FIGURE 5 Close-up of the frequency-shifted peak in the spectrum of the third harmonic generated in a 15 cm PCF by amplified Cr: forsterite laser pulses with an initial pulse duration of about 120 fs and an input energy of 40 nJ. The *insets* show typical third-harmonic intensity profiles at the output of the PCF corresponding to two orthogonal polarizations of the pump field at the input of the fiber

eralized to include the phase and group-velocity mismatch of the pump and third-harmonic fields as well as the Kerr-nonlinearity-induced spectral broadening of the pump field, tends to select a narrow spectral region of efficient THG. For pump fields with large nonlinear frequency deviations, this spectral region may lie several tens of terahertz away from the central frequency of the third harmonic $3\omega_0$. We have demonstrated that PCFs possess a unique combination of properties required to achieve large frequency shifts Ω , including dispersion tunability, maximum waveguide enhancement of nonlinear processes, and large interaction lengths. Photonic-crystal fibers are, therefore, ideally suited for an efficient tunable frequency up-conversion of ultrashort laser pulses based on frequency-shifted third-harmonic generation.

ACKNOWLEDGEMENTS We are grateful to Yu.N. Kondrat'ev, V.S. Shevandin, K.V. Dukel'skii, and A.V. Khokhlov for fabricating fiber samples. This study was supported in part by the President of Russian Federation Grant MD-42.2003.02, the Russian Foundation for Basic Research (project nos. 03-02-16929, 04-02-81036-Bel2004, 04-02-39002-GFEN2004, and 03-02-20002-BNTS-a), and INTAS (project nos. 03-51-5037 and 03-51-5288). The research described in this publication was made possible in part by Award no. RP2-2558 of the U.S. Civilian Research and Development Foundation for the Independent States of the Former Soviet Union (CRDF). This material is also based upon work supported by the European Research Office of the US Army under Contract No. 62558-04-P-6043.

REFERENCES

- 1 J.C. Knight, T.A. Birks, P.St.J. Russell, D.M. Atkin, *Opt. Lett.* **21**, 1547 (1996)
- 2 R.F. Cregan, B.J. Mangan, J.C. Knight, T.A. Birks, P.St.J. Russell, P.J. Roberts, D.C. Allan, *Science* **285**, 1537 (1999)
- 3 P.St.J. Russell, *Science* **299**, 358 (2003)
- 4 J.C. Knight, *Nature* **424**, 847 (2003)
- 5 C.M. Bowden, A.M. Zheltikov (eds.), *Nonlinear optics of photonic crystals*, *J. Opt. Soc. Am. B (Feature Issue)* **19**(9) (2002)
- 6 J.K. Ranka, R.S. Windeler, A.J. Stentz, *Opt. Lett.* **25**, 25 (2000)
- 7 W.J. Wadsworth, A. Ortigosa-Blanch, J.C. Knight, T.A. Birks, T.P.M. Mann, P.St.J. Russell, *J. Opt. Soc. Am. B* **19**, 2148 (2002)
- 8 A.M. Zheltikov (ed.), *Supercontinuum generation*, *Appl. Phys. B (Special Issue)* **77**(2/3) (2003)

- 9 X. Liu, C. Xu, W.H. Knox, J.K. Chandalia, B.J. Eggleton, S.G. Kosinski, R.S. Windeler, *Opt. Lett.* **26**, 358 (2001)
- 10 D. Akimov, M. Schmitt, R. Maksimenka, K. Dukel'skii, Y. Kondrat'ev, A. Khokhlov, V. Shevandin, W. Kiefer, A.M. Zheltikov, *Appl. Phys. B* **77**, 299 (2003)
- 11 D.A. Akimov, E.E. Serebryannikov, A.M. Zheltikov, M. Schmitt, R. Maksimenka, W. Kiefer, K.V. Dukel'skii, V.S. Shevandin, Yu.N. Kondrat'ev, *Opt. Lett.* **28**, 1948 (2003)
- 12 S.A. Diddams, D.J. Jones, J. Ye, S.T. Cundiff, J.L. Hall, J.K. Ranka, R.S. Windeler, R. Holzwarth, T. Udem, T.W. Hänsch, *Phys. Rev. Lett.* **84**, 5102 (2000)
- 13 D.J. Jones, S.A. Diddams, J.K. Ranka, A. Stentz, R.S. Windeler, J.L. Hall, S.T. Cundiff, *Science* **288**, 635 (2000)
- 14 R. Holzwarth, T. Udem, T.W. Hänsch, J.C. Knight, W.J. Wadsworth, P.St.J. Russell, *Phys. Rev. Lett.* **85**, 2264 (2000)
- 15 T. Udem, R. Holzwarth, T.W. Hänsch, *Nature* **416**, 233 (2002)
- 16 I. Hartl, X.D. Li, C. Chudoba, R.K. Rhanta, T.H. Ko, J.G. Fujimoto, J.K. Ranka, R.S. Windeler, *Opt. Lett.* **26**, 608 (2001)
- 17 S.O. Konorov, A.M. Zheltikov, *Opt. Express* **11**, 2440 (2003)
- 18 S.O. Konorov, D.A. Akimov, A.A. Ivanov, M.V. Alfimov, A.V. Yakimanskii, A.M. Zheltikov, *Chem. Phys. Lett.* doi: 10.1016/j.cplett.2005.01.127
- 19 A. Baltuska, T. Fuji, T. Kobayashi, *Opt. Lett.* **27**, 1241 (2002)
- 20 S.O. Konorov, D.A. Akimov, E.E. Serebryannikov, A.A. Ivanov, M.V. Alfimov, A.M. Zheltikov, *Phys. Rev. E* **70**, 057601 (2004)
- 21 H.N. Paulsen, K.M. Hilligsøe, J. Thøgersen, S.R. Keiding, J.J. Larsen, *Opt. Lett.* **28**, 1123 (2003)
- 22 D.V. Skryabin, F. Luan, J.C. Knight, P.St.J. Russell, *Science* **301**, 1705 (2003)
- 23 J.D. Harvey, R. Leonhardt, S. Coen, G.K.L. Wong, J.C. Knight, W.J. Wadsworth, P.St.J. Russell, *Opt. Lett.* **28**, 2225 (2003)
- 24 F. Benabid, J.C. Knight, G. Antonopoulos, P.St.J. Russell, *Science* **298**, 399 (2002)
- 25 S.O. Konorov, A.M. Zheltikov, P. Zhou, A.P. Tarasevitch, D. von der Linde, *Opt. Lett.* **29**, 1521 (2004)
- 26 D.G. Ouzounov, F.R. Ahmad, D. Müller, N. Venkataraman, M.T. Gallagher, M.G. Thomas, J. Silcox, K.W. Koch, A.L. Gaeta, *Science* **301**, 1702 (2003)
- 27 A.B. Fedotov, S.O. Konorov, V.P. Mitrokhin, E.E. Serebryannikov, A.M. Zheltikov, *Phys. Rev. A* **70**, 045802 (2004)
- 28 S.O. Konorov, E.E. Serebryannikov, D.A. Akimov, A.A. Ivanov, M.V. Alfimov, A.M. Zheltikov, *Phys. Rev. E* **70**, 066625 (2004)
- 29 S. Coen, A. H.L. Chau, R. Leonhardt, J.D. Harvey, J.C. Knight, W.J. Wadsworth, P.St.J. Russell, *J. Opt. Soc. Am. B* **19**, 753 (2002)
- 30 J.M. Dudley, L. Provino, N. Grossard, H. Maillotte, R.S. Windeler, B.J. Eggleton, S. Coen, *J. Opt. Soc. Am. B* **19**, 765 (2002)
- 31 N.I. Nikolov, T. Sørensen, O. Bang, A. Bjarklev, *J. Opt. Soc. Am. B* **20**, 2329 (2003)
- 32 J.K. Ranka, R.S. Windeler, A.J. Stentz, *Opt. Lett.* **25**, 796 (2000)
- 33 F.G. Omenetto, A. Taylor, M.D. Moores, J.C. Knight, P.St.J. Russell, J. Arriaga, *Opt. Lett.* **26**, 1558 (2001)
- 34 A. Efimov, A.J. Taylor, F.G. Omenetto, J.C. Knight, W.J. Wadsworth, P.St.J. Russell, *Opt. Express* **11**, 910 (2003)
- 35 A. Efimov, A.J. Taylor, F.G. Omenetto, J.C. Knight, W.J. Wadsworth, P.St.J. Russell, *Opt. Express* **11**, 2567 (2003)
- 36 F.G. Omenetto, A. Efimov, A.J. Taylor, J.C. Knight, W.J. Wadsworth, P.St.J. Russell, *Opt. Express* **11**, 61 (2003)
- 37 S.O. Konorov, A.A. Ivanov, M.V. Alfimov, A.B. Fedotov, Yu.N. Kondrat'ev, V.S. Shevandin, K.V. Dukel'skii, A.V. Khokhlov, A.A. Podshivalov, A.N. Petrov, D.A. Sidorov-Biryukov, A.M. Zheltikov, *Laser Phys.* **13**, 1170 (2003)
- 38 N. Naumov, A.B. Fedotov, A.M. Zheltikov, V.V. Yakovlev, L.A. Mel'nikov, V.I. Beloglazov, N.B. Skibina, A.V. Shcherbakov, *J. Opt. Soc. Am. B* **19**, 2183 (2002)
- 39 D.A. Akimov, A.A. Ivanov, A.N. Naumov, O.A. Kolevatova, M.V. Alfimov, T.A. Birks, W.J. Wadsworth, P.St.J. Russell, A.A. Podshivalov, A.M. Zheltikov, *Appl. Phys. B* **76**, 515 (2003)
- 40 G.P. Agrawal, *Nonlinear Fiber Optics* (Academic, Boston, 1989)
- 41 N.I. Koroteev, A.M. Zheltikov, *Appl. Phys. B* **67**, 53 (1998)
- 42 A.N. Naumov, A.M. Zheltikov, *Opt. Express* **10**, 122 (2002)
- 43 A.M. Zheltikov, *Optics of Microstructure Fibers* (in Russian) (Nauka, Moscow, 2004)
- 44 S.A. Akhmanov, A.P. Sukhorukov, A.S. Chirkin, *Zh. Eksp. Teor. Fiz.* **55**, 1430 (1968)